JSE Journal of Systematics and Evolution

doi: 10.1111/jse.70004

Research Article

Expelled by the Antarctic ice: Evolutionary history of the tribe Cunonieae (Cunoniaceae)

Francisco Fajardo-Gutiérrez[1,2]*, Mariasole Calbi[3], Markus S. Dillenberger[4], Sebastian Tello[5], Alfredo Fuentes[5,6], Nora H. Oleas[7], Ricardo A. Segovia[8,9], Christine E. Edwards[10], Yohan Pillon[11], James E. Richardson[12], and Thomas Borsch[1,4]

[1]Botanischer Garten und Botanisches Museum Berlin, Freie Universität Berlin, Berlin 14195, Germany
[2]Subdirección Científica, Jardín Botánico de Bogotá José Celestino Mutis, Bogotá 111071, Colombia
[3]Laboratory of Plant Biology, Department of Earth, Environment and Life Sciences, University of Genoa, Genoa 16132, Italy
[4]Institut für Biologie der Freien Universität Berlin, Berlin 14195, Germany
[5]Latin America Program, Missouri Botanical Garden, St. Louis 63110, MO, USA
[6]Herbario Nacional de Bolivia (LPB), Universidad Mayor de San Andrés, La Paz 10077, Bolivia
[7]Facultad de Ciencias del Medio Ambiente, Universidad Tecnológica Indoamérica, Ambato 120100, Ecuador
[8]Departamento de Botánica, Universidad de Concepción, Concepción 407038, Chile
[9]Instituto de Ecología y Biodiversidad, Concepción 7801806, Chile
[10]Center for Conservation and Sustainable Development, Missouri Botanical Garden, St. Louis 63110, MO, USA
[11]DIADE, Univ Montpellier, CIRAD, IRD, Montpellier 34394, France
[12]School of Biological, Earth and Environmental Sciences, University College Cork, Cork T23 N73K, Ireland
*Author for correspondence. E-mail: f.fajardo@bo.berlin
Received 5 March 2025; Accepted 6 June 2025

Abstract The tribe Cunonieae comprises five genera and 214 species of shrubs and trees currently distributed in the Southern Hemisphere and the tropics, exhibiting an amphi-Pacific disjunct distribution shared with Araucariaceae, Myrtaceae, Nothofagaceae, Podocarpaceae, and Proteaceae, among others. To address the central question of how historical geological forces have shaped the distribution of plant diversity in the southern hemisphere, we aimed to provide evidence from the biogeographical history of Cunonieae. We generated the most densely sampled phylogenetic trees of Cunonieae available to date, with 121 samples and 81 species, based on 404 new sequences of plastid and nuclear DNA regions with high hierarchical phylogenetic signal (*matK*, *trnL-F*, *rpl16*, and internal transcribed spacer (ITS)). We included 184 samples of Rosids to estimate divergence times using fossil calibration points. For biogeographic inference, we employed a time-stratified model including fossils as tips. *Cunonia* and *Pterophylla* were paraphyletic in the ITS tree, and *Cunonia* was paraphyletic in the plastid tree. *Pancheria*, *Vesselowskya*, and *Weinmannia* were monophyletic, the latter with conflicting nuclear and plastid phylogenies. The crown group Cunonieae was dated at ~56 Ma, and its ancestral areas were Antarctica and Patagonia. Antarctica acted as a bridge between Australia and South America before the consolidation of the Antarctic Ice Sheet and the extinction of the lineage in Antarctica from the Oligocene to the Miocene. Following that, Cunonieae spread to lower latitudes via Zealandia/Oceania and Patagonia/South America. Geological changes during the Pliocene facilitated a further burst in diversification along the Andes, in Madagascar, and in New Caledonia, where at least three colonization events occurred.

Key words: amphi-Pacific disjunction, ancestral ranges, Andes, Antarctica, biogeography, *Cunonia*, *Weinmannia*.

1 Introduction

Understanding the historical biogeography of lineages with disjunct distributions and how major paleogeographic events influenced the vicariance, dispersal, and extinction in these groups are fundamental topics of active research for evolutionary biology. For plants that have disjunct distributions across the southern hemisphere, early biogeographic theories focused on the effects of tectonic movements (Raven & Axelrod, 1972), Gondwanan biogeography (Anderson et al., 1999; McLoughlin, 2001), and Gondwanan breakup (Jokat et al., 2003). However, fossils indicate that angiosperm lineages of the Southern Hemisphere were also

affected by the formation of the Antarctic Ice Sheet (AIS) in the early Oligocene (approximately 34 Ma), at the final stages of the Gondwanan breakup (Cantrill & Poole, 2012; Kennedy et al., 2015). The opening of the Drake Passage between South America and Antarctica and the Tasman Seaway between Australia and Antarctica initiated the Antarctic circumpolar current, which contributed to the AIS formation (Kennedy et al., 2015). The AIS formation was a gradual process that began in the late Eocene in the central parts of Antarctica, expanding during the Oligocene and completing during the Miocene ~16 Ma (Cantrill & Poole, 2012). However, how the formation of the AIS affected the biogeography of plant lineages in the southern hemisphere is still poorly known.

Time-calibrated phylogenies of various plant lineages, for example, of Sapotaceae (Bartish et al., 2011), Loranthaceae (Liu et al., 2018), Alstroemeriaceae (Chacón et al., 2012), or Proteaceae (Barker et al., 2007), and genera like *Araucaria* Juss. (Rossetto-Harris et al., 2020), *Lomatia* R.Br. (Milner et al., 2015), *Nothofagus* Blume (Vento et al., 2024), and *Podocarpus* L′Hér. ex Pers. (Quiroga et al., 2016) have provided insights into the biogeography of plants that occur in the southern hemisphere. However, the major geological and climatic forces that drove the evolution of these lineages are still debated; for example, the Andean uplift was proposed to be important for *Podocarpus* and for Alstroemeriaceae, whereas the date of separation of South America from Antarctica was proposed to be relevant for the historical biogeography of *Araucaria*, *Nothofagus*, Loranthaceae, Proteaceae, and Sapotaceae. Antarctica might once have played a role as a migration route for terrestrial groups between the currently distant land masses of Australia and South America before the AIS formation. The ice sheet transformed the Antarctic continent from a forest landscape rich in woody angiosperms into a cold desert almost completely devoid of plants, thus effecting the biogeography of many plant clades occupying the southern hemisphere during its formation (Cantrill & Poole, 2012).

An ideal group to understand how historical forces have shaped the distribution of plant diversity in the southern hemisphere is the Cunoniaceae. Members of Cunoniaceae were present in the southern rainforest of Gondwana during the Eocene (Pujana et al., 2018) or upper Cretaceous (Pujana et al., 2025). Thus, Cunoniaceae is one of the Paleo Antarctic Rainforest Lineages (PARL), together with Araucariaceae, Myrtaceae, Nothofagaceae, Podocarpaceae, and Proteaceae (Tang et al., 2022). Cunoniaceae have a typical PARL distribution pattern, occurring in all the continents of the Southern Hemisphere, with the northernmost species occurring only as far north as Mexico, Cuba, Thailand, and the Philippines (see an up-to-date map in Pillon et al., 2021). Cunoniaceae comprises seven subfamilies, with one, Cunonioideae, further divided into seven tribes (Pillon et al., 2024). Here, we focus on the tribe Cunonieae Schrank & Mart., which includes 214 species classified in five genera: *Cunonia* L., *Pancheria* Brongn. & Gris, *Pterophylla* D.Don, *Vesselowskya* Pamp., and *Weinmannia* L. (Bradford & Barnes, 2001; Pillon et al., 2021). Cunonieae is the most species-rich tribe in the Cunoniaceae family (comprising two-thirds of the species of the family) and includes the most species-rich genus, *Weinmannia*, with 92 species according to Pillon et al. (2021), although the exact number of species has been disputed, due to difficult taxonomy and possible hybridization.

The distribution of extant Cunonieae spans Central and South America, Antilles, South Africa, Madagascar, Comoros, Mascarenes, Oceania, Malesia, and Eastern Australia (Barnes et al., 2001; Pillon et al., 2021). Because of its disjunct distribution across the South Pacific and the current high species diversity in tropical mountains, Cunonieae is a particularly relevant study group for investigating the biogeography of a group in the southern hemisphere. In addition, fossil representatives of the tribe found in Antarctica, Australia, Patagonia, and Tasmania (Barnes et al., 2001; Matel et al., 2022) offer opportunities to elucidate the major factors affecting the biogeography of plants in the southern hemisphere.

Cunonieae exhibits high diversity in the islands of the southern hemisphere. It is particularly diverse in New Caledonia, where three of the five genera occur; the main island "Grande Terre" hosts 55 endemic species of *Cunonia*, *Pancheria*, and *Pterophylla* in its 18 576 km^2. *Cunonia* comprises 25 species, 24 of which are endemic to New Caledonia and one is endemic to South Africa. *Pancheria* comprises 27 species, all endemic to New Caledonia. *Pterophylla* includes 68 species distributed in Southeast Asia (Thailand and Malesia), the South-West Pacific, and Madagascar, with many species restricted to islands. New Caledonia was submerged between 75 and 60 Ma, with a final re-emergence occurring between 34 and 25 Ma (Maurizot & Campbell, 2020). This would imply that the archipelago is a "Darwinian island" defined as an oceanic island with biota dominated by neoendemism and a history of disharmonic colonizations. Studies on molecular dating of New Caledonian endemic clades are consistent with this scenario (Bartish et al., 2005; Cruaud et al., 2012; Pillon, 2012; Nattier et al., 2017).

In the Andean regions of South America, many *Weinmannia* species have restricted ranges, and 40 out of 91 species are found in only one country (León, 2006; Morales, 2010). The uplift of the Andean cordillera began in the Paleogene (65–34 Ma), but it was only during the late Miocene (10–6 Ma) that these tropical mountains reached sufficient heights (~3000 m) to allow conditions appropriate for the formation of widespread paramo and cloud forest ecosystems (Madriñán et al., 2013; Boschman, 2021), where *Weinmannia* is a species-rich and often dominant component (González-Caro et al., 2023). In the context of Andean orography, *Weinmannia*, together with *Podocarpus* (Podocarpaceae), *Drimys* J.R.Forst. & G.Forst. (Winteraceae), and *Bomarea* Mirb., (Alstroemeriaceae) were hypothesized to have moved northward along the Andes (Chacón et al., 2012; Segovia & Armesto, 2015).

Previous attempts to understand the evolutionary history of Cunoniaceae employed plastid and nuclear markers (Bradford & Barnes, 2001; Pillon et al., 2009a, 2009b). Recently, Pillon et al. (2021) conducted a complete sampling of genera and employed a target sequence capture approach to elucidate the phylogenetic relationships within the family using the Angiosperms353 bait set (Johnson et al., 2019). Based on a set of 14 genes that were consistently retrieved across their samples, Pillon et al.

(2021) estimated the divergence age between the Codieae and Cunonieae stems at 52.8 Ma [54.6–51.0 Ma] in the early Eocene, whereas the divergence of the crown group of Cunonieae (*Cunonia*, *Pancheria*, *Pterophylla*, and *Weinmannia*) was calculated at 32.3 Ma [34.4–30.2 Ma], during the Oligocene. This suggests that the origin of the disjunct distribution patterns of extant Cunonieae in the Southern Hemisphere cannot be explained by vicariance during the breakup of Gondwana alone, which began much earlier, about 180 Ma (McLoughlin, 2001). Based on this phylogeny, Pillon et al. (2021) transferred all sections of *Weinmannia sensu lato* to *Pterophylla* except section *Weinmannia* (sensu Bradford, 1998), and we follow this updated infrageneric classification of sections of *Pterophylla*. However, Pillon et al. (2021) included only 10 of the 214 total Cunonieae species and only two of the 92 species of *Weinmannia* section *Weinmannia*, sensu Bradford (2002): *Weinmannia pinnata* L. and *W. tinctoria* Sm. Therefore, more complete sampling of all major distribution areas across the Cunoniae genera is needed to test the monophyly of the genera and elucidate the biogeography of the group.

To address the central scientific question of how historical geological forces have shaped the distribution of plant diversity in the southern hemisphere and to provide evidence from an outstanding biological model, we aimed to develop a detailed reconstruction of the biogeographical history of Cunonieae. We hypothesized that the modern distribution of the tribe was influenced by the expansion of the AIS, which could have expelled Cunonieae lineages from the Antarctic continent through extinction, vicariance, and dispersal events. This could have been followed by the diversification of the genera in the Tropical Andes, New Caledonia, Madagascar, and from the South Pacific to the Thailand Peninsula. We set out to answer four specific questions: i) Do the genera of Cunonieae remain monophyletic when phylogenies have greater taxon sampling? ii) Is the timing of divergences associated with changes in continental landmasses (i.e., the AIS formation and Andean uplift)? iii) What role has Antarctica played in shaping the current distribution of Cunonieae across the Southern hemisphere? And iv) What is the relative importance of vicariance, long-distance dispersal, speciation, and extinction in explaining the modern distribution and diversity of Cunonieae?

2 Material and Methods

2.1 Taxon sampling

Our data set included 193 samples representing 159 species in total: 85 samples in the ITS matrix and 184 samples in the plastid markers matrix, with an overlap of 76 samples present in both data sets (Table S1). We produced 404 new sequences from newly extracted DNA of 98 species, whereas we obtained sequences of 78 samples from previously published phylogenetic works (Bradford, 2002; Foster et al., 2017; Li et al., 2021; Pillon et al., 2021; Wang et al., 2023; a list of additional references is available in the Supporting Information in "Additional references for GenBank accessions in Table S1"). Within Cunonieae, we worked with 121 samples corresponding to 81 species, including 21 species of *Pancheria* (77.8% of the accepted number of species), 16 species of *Cunonia* (64%), one species of *Vesselowskya* (50%), 40 species of *Weinmannia* (43.5%), and seven species of *Pterophylla* (10.3%), collected along the natural distribution of the clades (Fig. S1). For outgroups, we included representatives of three subfamilies of Cunoniaceae and five of the seven tribes of subfamily Cunonioideae (Pillon et al., 2024). To enable fossil calibration (Foster et al., 2017), we included representatives of five other families in the Oxalidales, Celastrales (Celastraceae and Parnassiaceae), and Malpighiales (Euphorbiaceae, Malpighiaceae, Passifloraceae, and Salicaceae), as well as five more orders within the Rosids: Cucurbitales, Fabales, Fagales, Rosales, and Zygophyllales (Foster et al., 2017). All the samples used have reference specimens in the following herbaria: B, JBB, JAUM, LPB, MO, NOU, and P, acronyms following Thiers (2025, updated continuously) (Table S1). TROPICOS website (https://tropicos.org—Missouri Botanical Garden) was used to find herbarium specimens with tissue material available, and JSTOR Global Plants (http://plants.jstor.org) was used to identify plant material from field work and herbarium.

2.2 Molecular laboratory methods

DNA isolation was carried out from silica-dried leaf material and herbarium specimens using the NucleoSpin Plant II extraction kit (Macherey Nagel, Düren, Germany), the triple cetyltrimethylammonium bromide (CTAB) extraction method (Borsch et al., 2003), or a modified CTAB method with a Sorbitol prewash step (Inglis et al., 2018). Sequences of the *matK-trnK-psbA*, *trnL–trnF*, and *rps3–rpl16* plastid regions and the nuclear ITS were obtained by PCR amplification using the primers *trnKF* and *psbA5R* (Wicke & Quandt, 2009), *trnTc* and *trnTf* (Taberlet et al., 1991), *rpl16R* and *rpl16F* (Campagna & Downie, 1998), and ITS4 and ITS5 (White et al., 1990), respectively. Four new primers were designed; specifically, two for the *matK-trnK-psbA* region (CUNmatK541F: 5′-CTTCTTTGCATTTATTACGG-3′ and CUNmatK624R: 5′-AGGAA CAAGAATAATCTTGG-3′) and two for the *rps3–rpl16* region (OXAL_rps3_55R: 5′-TWGTTCCTATACAGTTAGAAC-3′ and OXAL_rpl16-1242F: 5′-TTCGTGTCATTGCTCGTCGC-3′). Sanger sequencing was performed at Macrogen Europe B.V. (Amsterdam, the Netherlands), and the resulting electropherograms were visually inspected for erroneous nucleotide callings and assembled using PhyDe v. 0.9971 (Müller et al., 2005). A total of 404 new sequences were generated, 329 for plastid markers and 75 ITS sequences (Table S1).

2.3 DNA alignment and phylogenetic analysis

We followed a motif-alignment approach (Löhne & Borsch, 2005) using PhyDE (Müller et al., 2005), retrieving an initial alignment comprising 185 samples at 8906 characters of concatenated plastid markers. We removed regions of uncertain homology such as mutational hotspots and poly A/T microsatellites. In that way, we obtained a final matrix of 7909 characters, of which 6619 were DNA and 1290 were binary-coded indels, with 6.59% missing data. Insertions and deletions were coded with SeqState 1.40 (Müller, 2005a) using simple indel coding (Simmons & Ochoterena, 2000). An inversion of six nucleotides in the 3′ end of the *trnK* intron in six samples of Celastraceae was reverse-complemented and coded in the indel matrix (positions 3833–3871 of the DNA

matrix). A map with the collection localities of the 127 Cunoniaceae samples sequenced at plastid markers is shown in Fig. S1, differentiating between GenBank accessions and new sequences; outgroups of other families are not included in this figure. A separate DNA matrix with a set of 86 samples comprising only Cunonieae (75 new sequences) was created for ITS (ITS alignment in Supplementary material). This sampling allowed us to align the ITS sequences with reliable homology, which was not feasible at the Oxalidales or Rosids level because of the high variability of the region. ITS and plastid alignments are available as Supplementary material: Cun_ITS_alignment.nex and Cun_plastid_alignment.nex (Fajardo, 2024a). GenBank accession numbers are listed in Table S1.

We conducted phylogeny reconstruction on both the ITS and plastid data sets using three approaches. Maximum parsimony trees were inferred with the program PAUP v. 4.0a (Swofford, 2002) with the following settings: 200 ratchet iterations with 25% of the positions randomly up-weighted (weight = 2) on each iteration, plus 20 random additional cycles, using commands generated in PRAP v. 1.21 (Müller, 2004). The nexus file was analyzed in PAUP using heuristic searches and tree bisection-reconnection branch swapping. Jackknife values were also calculated in PAUP with 100 000 pseudo-replicates, and 36.79% of the characters were deleted at each replicate (Müller, 2005b). A maximum likelihood analysis was performed using RAxML-NG v. 1.0.2 (Kozlov et al., 2019). Transfer Bootstrap Expectation support (TBE) was estimated based on the majority-rule consensus tree from 1000 replicates (Lemoine et al., 2018). MrBayes v. 3.2.7 (Ronquist et al., 2012) was used to calculate Bayesian trees. The nucleotide substitution models for each partition were estimated during the Bayesian analysis using bModelTest (Bouckaert & Drummond, 2017; Table S2), as implemented in MrBayes. Analyses were performed with four runs of Monte Carlo Markov Chains (MCMC) with four parallel chains each. We performed 10 million generations per chain, sampling every 10 000 generations, with a burn-in fraction of 25%. The resulting MrBayes consensus tree (Figs. 1, S2, S3) was visualized and edited, combining parsimony support JackKnife (JK), maximum likelihood bootstrap (TBE), and posterior probability (PP) from MrBayes, in TreeGraph2 (Stöver & Müller, 2010). We interpreted PP values of <0.9 as not supported, 0.9 to 0.94 PP as weakly supported, and 0.95 to 1.0 PP as well-supported nodes. All the phylogenetic analyses were computed in the Curta high performance computing cluster of the FU Berlin (Bennett et al., 2020).

2.4 Divergence time estimation

The plastid tree was employed for time calibration and biogeographic reconstruction because it allowed us to align samples from different families and orders with high sequence homology, allowing us to include well-known Rosid fossil calibration points (Foster et al., 2017; Table S3). We tested the effects of Yule's speciation model versus the Birth-Death model (BDM) as branching process priors using the BEAST package "Model-Selection" v. 1.4.2, which performed a stepping-stone sampling with 150 steps, chain lengths of 100 000 iterations, 80% burn-in percentage, preburning of 50 000 samples, and alpha parameter of 0.3. The model's marginal likelihood estimates favored the BDM over Yule's model, with a Bayes Factor of 816.7 (Lartillot & Philippe, 2006).

First, we estimated the age of the crown node of Cunoniaceae to be used as a secondary calibration point at the root prior of Cunoniaceae in a subsequent analysis, using nine fossil records assigned to Fabales, Fagales, Malpighiales, Oxalidales, and Rosales (Fig. S4; Table S3). To do this, a subset of 65 samples (5.06% of missing data) was first used, dropping 93 tips of the plastid tree, including 69 tips of the Cunonieae tribe (Table S4, scenarios A & B). This balanced tree topology (Fig. S4) allowed us to avoid the possible bias caused by the overrepresentation of *Cunonia*, *Pancheria*, and *Weinmannia* (Duchêne et al., 2015). The Cunoniaceae fossils used in the divergence time estimation were: *Ceratopetalum suciensis* Tang & Atkinson; *Codia australiensis* R.W.Barnes & R.S.Hill; *Racemofructus fasciculatus* Matel, Gandolfo, Hermsen & Wilf; *Pterophylla* sp. (Barnes, 1999); and *Weinmannia potosina* (Britton) Berry. The *Pterophylla* sp. was described as "*Weinmannia* indet. sp. (specimen WC-236) from Wilson's Creek, central Tasmania" based on its cuticular features, stomata, and trichomes (Barnes, 1999, figs. 6.5 to 6.9 of his Chapter 6), which were compared with the extant taxa *Pterophylla bojeriana* (Tul.) J.Bradford & Z.S.Rogers, *Pterophylla richii* (A.Gray) Pillon & H.C.Hopkins, *Pterophylla serrata* (Brongn. & Gris) Pillon & H.C.Hopkins, and *Pterophylla sylvicola* (Sol. ex A.Cunn.) Pillon & H.C.Hopkins. These four names were transferred from *Weinmannia* to *Pterophylla* after the description of the fossil (Pillon et al., 2021). For this reason, and for the nonexistence of confirmed extant (or fossil) records of *Weinmannia* s.s. in Asia or Oceania, we decided to use this fossil as *Pterophylla* sp. (Table S3). Additional references of fossil descriptions, dating, and placement are presented in the Supporting Information, Tables S3 and S5.

Divergence times were estimated with BEAST v. 2.5.2 (Bouckaert et al., 2019). For the estimation of divergence times, we used an uncorrelated relaxed clock log-normal (Drummond et al., 2006), a BDM, 10 million generations, sampling every 10 000 generations, with a preburning of 2.5 million generations. This resulted in a 95% highest posterior density (HPD) of the crown Cunoniaceae node estimated at 80–88.9 Ma.

Second, a set of 84 samples (6.35% of missing data) representing only Cunoniaceae plastid data was time-calibrated with BEAST under the same parameters, with a root prior of [80–88.9 Ma] estimated in the previous analysis (Table S4, scenarios C to F). Five Cunoniaceae fossils were used for this time-calibration: *Ceratopetalum suciensis*, *Racemofructus fasciculatus*, *Codia australiensis*, *Weinmannia potosina*, and "*Weinmannia* indet. sp." (Barnes et al., 2001), the latter of which is revised here as *Pterophylla* sp. (Table S3). To account for the uncertainty of placement of the ingroup fossils *Pterophylla* sp. and *Weinmannia potosina*, four scenarios were explored with different placements of the two fossils (Table S4, scenarios C, D, E, and F). The C scenario was selected based on the effective sample size (ESS) of the likelihood estimation, as a measure of the effectiveness of the MCMC analysis for each parameter in BEAST (Table S4; Bouckaert et al., 2019), with *Pterophylla* sp. at the crown

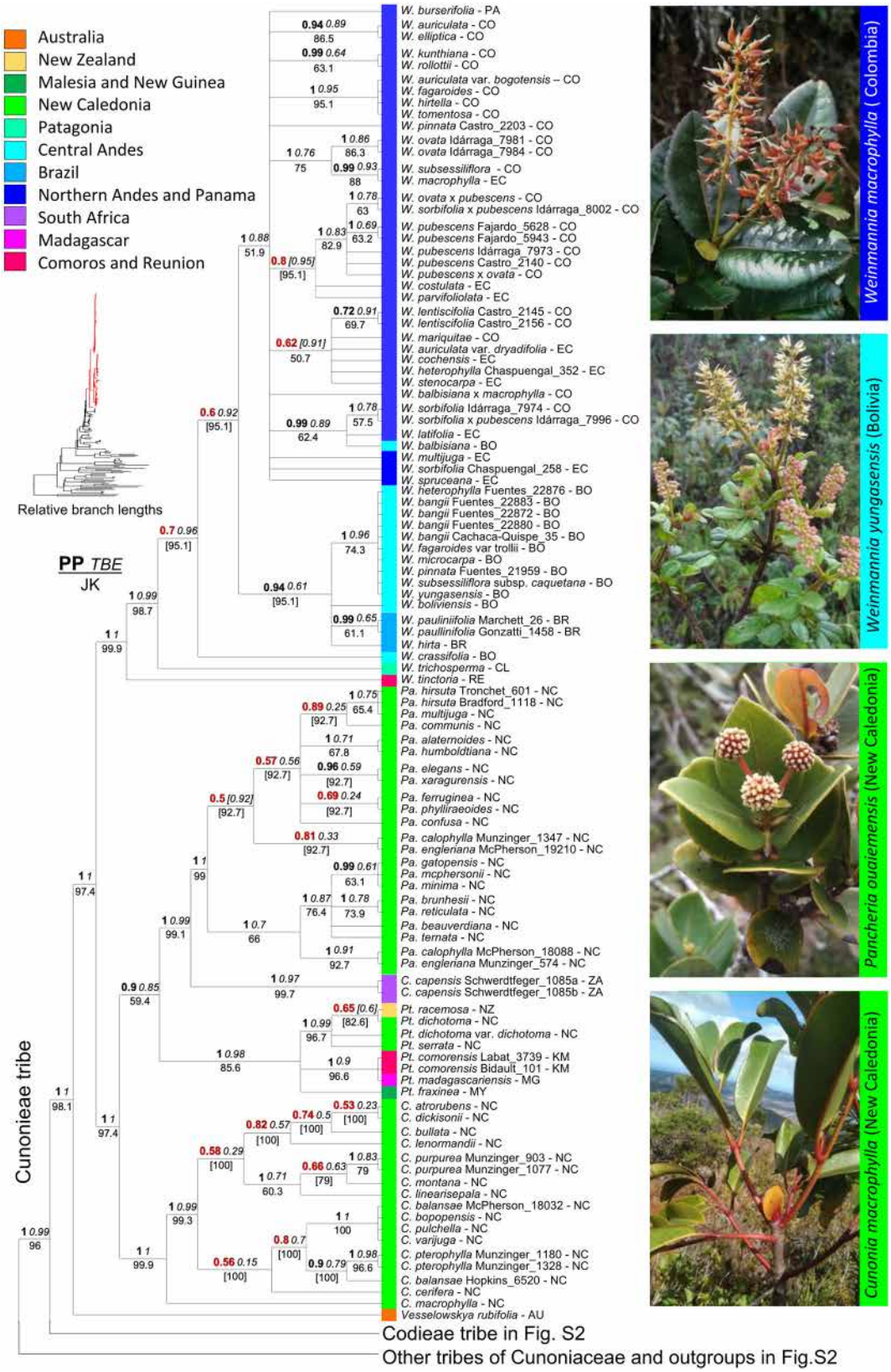

Fig. 1. Continued

node of *Pterophylla* and *W. potosina* at the crown node of the Tropical Andes *Weinmannia*, at the divergence of *Weinmannia crassifolia* Ruiz & Pav. (Figs. 2, 3).

The convergence of BEAST′s output was analyzed using Tracer v. 1.7.2 (Rambaut et al., 2018) using the ESS. The tree file with 1000 stored trees was summarized into a maximum clade credibility tree, with a post-burn-in percentage of 25% using TreeAnnotator v. 2.5.2 (Drummond & Rambaut, 2007). The 95% HPD intervals of node ages and median heights were calculated from 751 post-burn-in trees. Finally, a plot of lineages through time (LTT) was visualized with the R package Ape (Paradis & Schliep, 2019). Scripts, XML files for BEAST parameters, and results of every time calibration scenario are available in Figshare (Fajardo, 2024b).

2.5 Ancestral range reconstruction

We used the Cunoniaceae time-calibrated tree from BEAST to conduct ancestral range reconstructions with a particular focus on the tribe Cunonieae. We used the continents, land masses, or islands that species currently occupy as areas, except South America, which was divided into Brazil, Central Andes, Northern Andes, and Patagonia. Mascarenes, Samoa, and Comoros were grouped as volcanic islands of <10 Ma, unavailable as ancestral areas before their volcanic emergence, and with one sample each that in all three cases requires a long-distance dispersal event for arrival. Antarctica, North America, and Tasmania were also included, accounting for the occurrence of Cunoniaceae fossils (Tables S3, S5). A total of 13 fossils were used for the ancestral range reconstruction (Fig. 3; Table S5). All fossils were inserted as tips at the age of the record (Wood et al., 2013), with a terminal branch length of 0.1 Ma in TreeGraph2 (Stöver & Müller, 2010). We carried out a time-stratified analysis using BioGeoBEARS (Matzke, 2013), comparing the *dispersal-extinction-cladogenesis* DEC, DEC + J, DIVALIKE, DIVALIKE + J, BAYAREALIKE, and BAYAREALIKE + J models (Matzke, 2014), with "J" representing the "jump dispersal" (Matzke, 2014; Ree & Sanmartín, 2018). The time boundaries (Tables S6, S7) were established with the following criteria:

1) The uplift of the Northern Andes (Boschman, 2021): 16–0 Ma.
2) The final re-emergence of New Caledonia (Maurizot & Campbell, 2020): 25–16 Ma.
3) The AIS formation (Cantrill & Poole, 2012; Kennedy et al., 2015): 34–25 Ma.
4) The separation of Tasmania from Antarctica and Australia (McLoughlin, 2001): 60–34 Ma.
5) The maximum estimated age of Cunoniaceae according to our time calibration and Zuntini et al. (2024): 100–60 Ma.

For each period, we set up a matrix of "dispersal multipliers" (de la Estrella et al., 2019), a matrix of "areas allowed," and a matrix of "areas adjacency" (Matztke, 2014). We used 14 areas and 94 tips (Tables S6). The maximum number of areas a species may occupy was set to 3. The R script of BioGeoBEARS, input time-calibrated phylogeny with the fossils applied as tips, and all the parameters of the ancestral range reconstruction models are available in Figshare (Fajardo, 2024c) and in Tables S6 to S11.

3 Results

3.1 Phylogenetic relationships within the Cunonieae tribe

Overall, the plastid tree has strong support for nodes along the backbone of the phylogeny but less support for relationships among species. In the plastid tree, both Cunoniaceae and the tribe Cunonieae were recovered as monophyletic with PP = 1.0, with Codieae as a sister clade to Cunonieae (Figs. 1, S1). In Cunonieae, *Vesselowskya* was placed as the sister to the remainder of Cunonieae, which was divided into two clades, one strongly supported clade including all *Weinmannia* and another including all the remaining genera. Within the latter group, clades composed of (i) *Cunonia* (except *Cunonia capensis* L.), (ii) *Pterophylla,* and (iii) two accessions of *C. capensis* were placed as successive sisters to *Pancheria*, making *Cunonia* a paraphyletic group. The genera *Pancheria*, *Pterophylla*, and *Weinmannia* each formed monophyletic groups with strong support (PP = 1.0) in the plastid tree. Some polytomies occurred within *Pancheria* and among Andean *Weinmannia*, where nodes were collapsed below the threshold of PP = 0.2 (Fig. 1). Within *Weinmannia*, *Weinmannia tinctoria* Sm. from Réunion and Mauritius (PP = 1.0), *W. trichosperma* Cav. From Chile, and *W. crassifolia* from Bolivia were successive sister groups (PP = 1.0) to the remainder of the Andean and Brazilian species (Fig. 1), the latter of which was supported by bootstrap (TBE = 0.92), but with no support on MrBayes (PP = 0.6). Andean *Weinmannia* was divided into two groups, one containing the species from Bolivia and Brazil, including *W. boliviensis* R.E.Fr. (PP = 0.94), and the other containing species from Colombia and Ecuador (PP = 1.0), with one sample from Bolivia and one sample from Panama (Fig. 1).

In the ITS tree, *Pterophylla* was paraphyletic (Fig. S3), with one clade from Comoros and Madagascar (PP = 0.98) sister to the remaining *Pterophylla* species from Oceania and Malesia, *Cunonia* and *Pancheria*. *Cunonia* was retrieved as paraphyletic in the ITS tree, with *C. capensis* and *Cunonia macrophylla* Brongn. & Gris placed as a sister group to the remaining *Cunonia* plus *Pancheria* (Figs. S3, S5). In

Fig. 1. Phylogeny of Cunonieae based on *matK*, *trnL-F*, and *rpl16*. *C.* = *Cunonia*, *Pa.* = *Pancheria*, *Pt.* = *Pterophylla*, *W.* = *Weinmannia*. The two letters at the end of the scientific names are Alpha-2 code of the country of the collection event following the ISO 3166 international standard. Support values are given on the subtending branch of each node: on top PP = posterior probability [bold], and TBE = Transfer Bootstrap Expectation [*italics*], and JK = Jackknife below the line. The topology shown resulted from the Bayesian analysis; support values in square brackets were not identically recovered by the maximum likelihood or the parsimony analyses, PP values in red (<0.9) are considered as not supported. Other Cunoniaceae tribes and outgroups continue in Fig. S2. Field pictures: *W. macrophylla* (photo credit: Diego M. Cabrera), *W. yungasensis* (photo credit: Alfredo Fuentes), *C. macrophylla* and *Pa. ouaimensis* (photo credit: Francisco Fajardo).

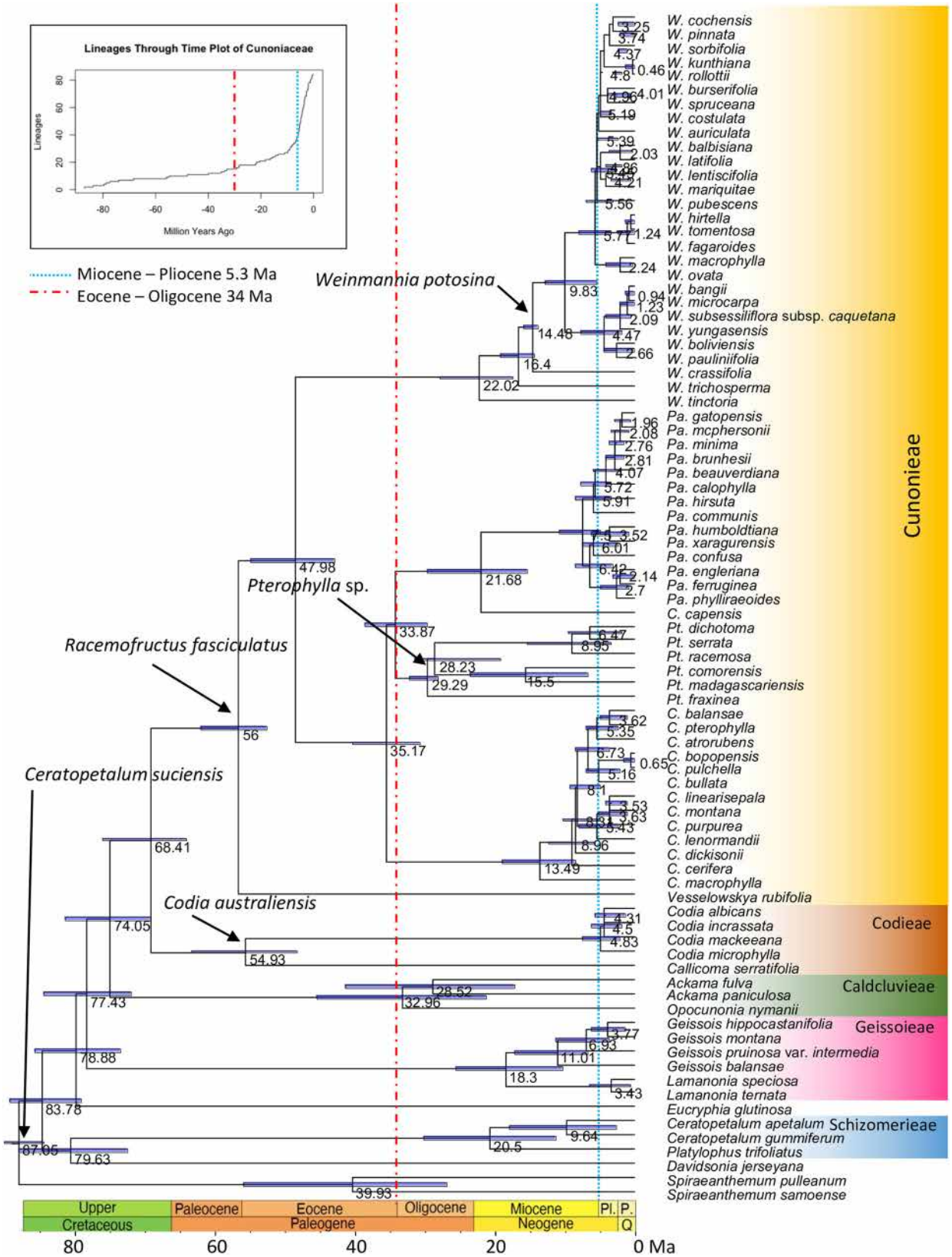

Fig. 2. Maximum clade credibility tree of Cunoniaceae showing the placement of five out of nine fossil calibration points (Tables S3, S4, scenario C) and the 95% highest posterior density (HPD) intervals. Age of the fossil calibration points: *Weinmannia potosina* = 13.8 Myr, *Pterophylla* sp. = 27.8 Myr, *Codia australiensis* = 47.8, *Racemofructus fasciculatus* = 52 Myr, and *Ceratopetalum suciensis* = 80 Myr. The lineages through time plot show a steep increase in lineages from the Pliocene onward.

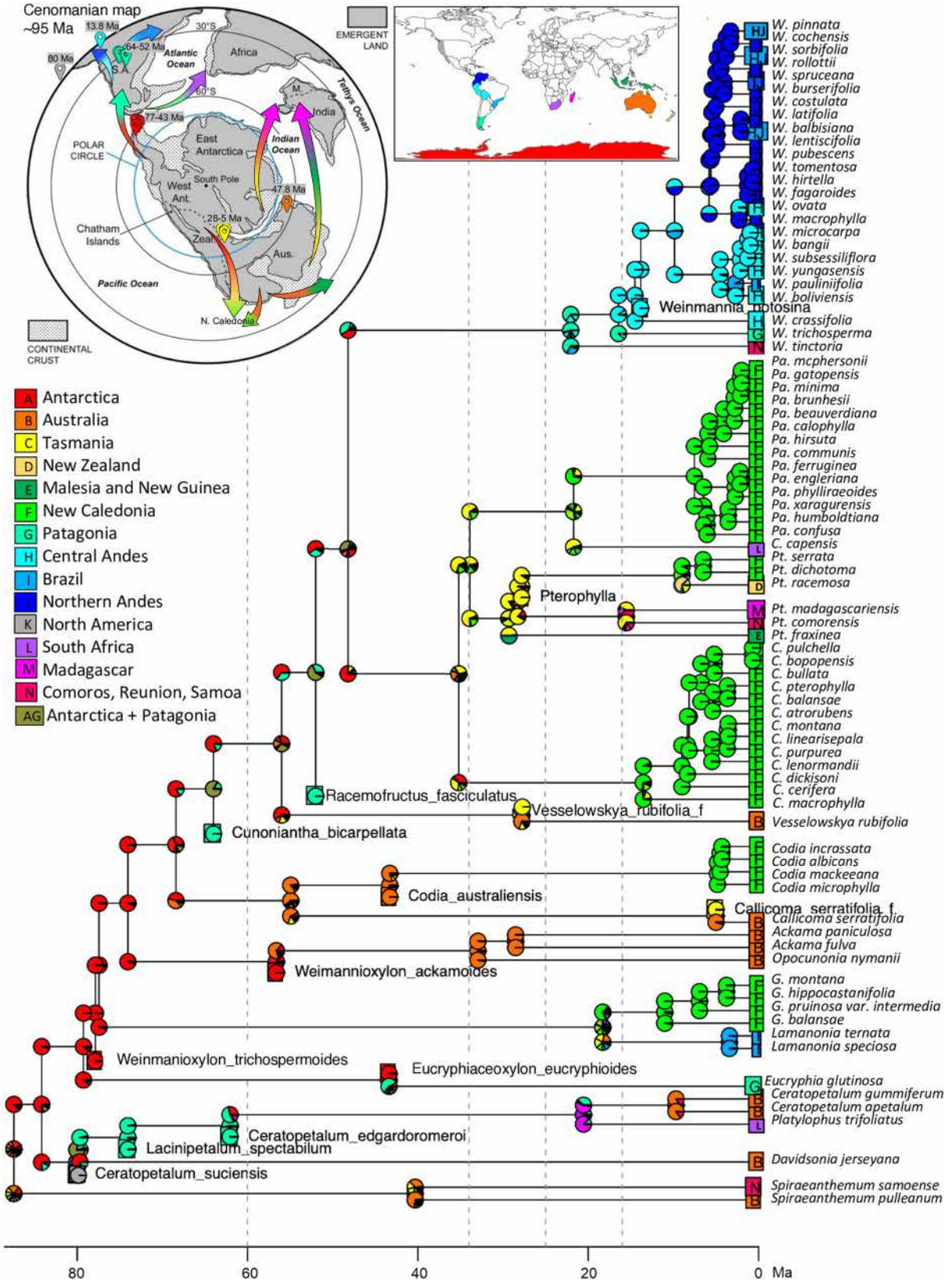

Fig. 3. Continued

Weinmannia, *W. trichosperma* and *W. boliviensis* were successive sisters to the rest of *Weinmannia* (PP = 0.99), and *W. tinctoria* from Réunion was placed in the northern Andes clade (Fig. S3). The detailed comparison between plastid and nuclear ITS trees is shown in Figs. S5 and S6.

3.2 Divergence time estimation

The diversification of the crown node Cunoniaceae was dated to 87.05 Ma [95% HPD 80.5–88.9 Ma] in the upper Cretaceous. The stem node of Cunonieae diverged from Codieae at 68.4 [63.3–75.3 Ma] and began diversifying at the divergence of *Vesselowskya* at 56.0 Ma [52–61.2 Ma], in the Paleocene–Eocene transition. During the Eocene, we find long branches and the divergence (~48 Ma) between western (modern *Weinmannia*) and eastern Cunonieae (modern *Cunonia*, *Pancheria*, and *Pterophylla*). During the Oligocene, *Pterophylla* began diversifying, and during the Miocene, *Cunonia*, *Pancheria*, and *Weinmannia* began diversifying (Fig. 2; Table 1). The LTT plot (Fig. 2) shows a steep increase in the number of lineages beginning in the Pliocene.

3.3 Ancestral range reconstruction

The model with the best performance in the BioGeoBEARS analysis was DIVALIKE with a natural Log of Likelihood (LnL) = −210.21, with the parameters $d = 0.0105$ (dispersal), $e = 0.0183$ (extinction), $j = 0.0$ (jump dispersal), and AIC = 424.4 (Fig. 3). The DEC and BAYAREALIKE models performed slightly worse (Table 2), although the geographical ranges recovered were mostly like those of DIVALIKE. The addition of parameter J (DIVALIKE + J and DEC + J) resulted in better LnL values (Table 2), but the jump dispersal (*J*) in this intercontinental scale allowed too many long-distance dispersal events, skipping the adjacency matrix completely, often resulting in disjunct ranges along the phylogeny. Additionally, Ree & Sanmartin (2018) showed that BioGeoBEARS always favors +J models over those without +J, which is another reason to choose the DIVALIKE model without +J.

The most important ancestral area recovered for Cunoniaceae phylogeny was the Antarctic, followed by Patagonia, Tasmania, and Australia (Fig. 3). Cunonieae originated in Antarctica and Patagonia, modern *Weinmannia* followed the pathway from Antarctica–Patagonia–Central and Northern Andes, whereas the remaining genera followed the pathway from Antarctica–Tasmania–Australia–Zealandia–New Caledonia and other islands. *Pancheria* and most *Cunonia* originated in New Caledonia (Fig. 3).

4 Discussion

4.1 Phylogenetic relationships and monophyly of Cunonieae genera

The relationship between Cunoniae and other Cunoniaceae tribes is generally consistent with results from previous studies. Our plastid tree (Figs. 1, S1) exhibited the same overall topology with high support within Cunoniaceae as the nuclear phylogenomic tree of Pillon et al. (2021), in which the Schizomerieae, Geissoieae, Caldcluvieae, and Codieae were placed as successive sister groups to Cunonieae. Whereas in the tree of Pillon et al. (2021), *Davidsonia*, subfamily Davidsonioideae, was sister to the subfamily Schizomerioideae, the same as in our time-calibrated tree (Figs. 2, 3, PP = 0.92), in the plastid tree, *Davidsonia* was placed in a grade branching after the Schizomerioideae clade (Fig. S2, PP = 0.89).

Table 1 Estimated time of occurrence of some important events of Cunonieae evolution, obtained from the time-calibration analysis of the plastid phylogeny in BEAST2

Clade	Node age (Ma)	95% HPD range (Ma)	Event referred
Cunoniaceae	87.05	88.9–80.5	Crown Cunoniaceae
Cunonieae tribe	68.41	75.3–63.3	Stem age of Cunonieae tribe
Cunonieae tribe	56.0	61.2–**52.0**†	Crown node Cunonieae tribe, divergence of *Vesselowskya*
Cunonieae tribe	47.98	54.28–42.3	Stem age of *Weinmannia*
Weinmannia	22.02	27.55–17.34	Crown node of *Weinmannia* (Mascarenes species)
Weinmannia	16.4	18.91–14.14	Crown node of South American species
Weinmannia	14.48	15.79–**13.8**†	Crown node of Central Andes species (*W. crassifolia*)
Weinmannia	9.83	12.61–5.28	Crown node of Central and Northern Andes species
Cunonieae tribe	35.17	39.97–30.33	Crown node of *Cunonia* + *Pancheria* + *Pterophylla* Clade
Pterophylla	29.29	31.83–**27.8**†	Crown node of *Pterophylla* (widespread *Pterophylla fraxinea*)
Cunonia	13.49	18.68–8.47	Crown node of New Caledonian *Cunonia*
C. capensis	21.68	29.4–15.25	Divergence of *C. capensis* from the stem node of *Pancheria*
Pancheria	7.5	10.61–4.89	Divergence from *C. capensis*

HPD = highest posterior density; †Points where fossil calibration was applied, the estimated age of each fossil is in bold.

Fig. 3. Major routes of dispersion are depicted over the palaeogeographical reconstruction from a polar perspective, at the Cenomanian (~95 Ma), reproduced with authorization from Mays et al. (2015): colored arrows represent the areas from which clades of Cunonieae have migrated, location and age of fossils are shown in the same color palette (Table S5). Ancestral range reconstruction of Cunonieae and related Cunoniaceae. Time stratified DIVALIKE model with *max_areas* = 3, $d = 0.0105$, $e = 0.0183$, $j = 0$, LnL = −210.21. *C.* = *Cunonia*, *G.* = *Geissois*, *Pa.* = *Pancheria*, *Pt.* = *Pterophylla*, and *W.* = *Weinmannia*.

Table 2 Results of the BioGeoBEARS comparison of models. The DIVALIKE model was chosen based on the natural log likelihood (LnL) and accounting for the intercontinental scale of the analysis

	LnL	Number of parameters	*d* (dispersal)	*e* (extinction)	*j* (jump dispersal)
DEC	−212.0809	2	0.009711154	0.020900459	0.00
DEC + J	−185.5045	3	0.002689790	0.004817502	0.03256895
DIVALIKE	−210.2081	2	0.010489972	0.018330222	0.00
DIVALIKE + J	−182.5015	3	0.003236295	0.004667128	0.02779031
BAYAREALIKE	−248.3967	2	0.012123163	0.040963637	0.00
BAYAREALIKE + J	−190.1575	3	0.001915888	0.004857502	0.03851930

For Cunonieae, our study contains 81 out of 214 species currently accepted by Pillon et al. (2021) in the five genera (39.7%) and thus presents the most comprehensive phylogeny for the tribe so far, particularly for *Weinmannia*, which shows some interesting biogeographic patterns. Whereas Pillon et al. (2021) included only two *Weinmannia* species (*Weinmannia pinnata*, *W. tinctoria*), with its greater taxon sampling (40 sampled species out of 92 species in total), the present study shows for the first time that *Weinmannia* is monophyletic, comprising 90 American species plus two species from the Mascarene Islands (*Weinmannia mauritiana* D. Don and *W. tinctoria*). In both the ITS and plastid phylogenies, *W. trichosperma* from Chile holds an early branching position (Fig. S3). *Weinmannia trichosperma* is the only temperate *Weinmannia* species, whereas other species are tropical but occupy high elevations; thus, understanding *Weinmannia* climatic preferences could be an interesting future avenue of study.

Even though the placement of some *Weinmannia* taxa is similar between the ITS and plastid phylogenies, within *Weinmannia*, many relationships also differ (Fig. S5). For example, in the plastid tree, the Mascarene species *W. tinctoria* is placed as sister to the remainder of *Weinmannia* and all the American *Weinmannia* species form a well-supported clade (PP = 1.0), whereas the ITS tree places *W. tinctoria* as nested within the northern Andes clade (PP = 0.99) (Figs. S3, S5, S6). Similarly, *W. boliviensis* is at the base of *Weinmannia* in our ITS tree as sister to *W. trichosperma* (not supported by MrBayes PP = 0.6, but supported by RaxML TBE = 0.97), whereas in the plastid tree, *W. boliviensis* is placed in a Bolivian and Brazilian clade (PP = 0.94). This incongruence between ITS and plastid trees may be the result of reticulate evolution (Martin et al., 2005) as evidenced by conflict between biparentally inherited nuclear DNA versus the maternally inherited line of the plastid tree. Furthermore, the occurrence of multiple ITS copies as observed in some *Weinmannia* electropherograms during our lab work can be common in Cunoniaceae (Bradford, 2002; Hopkins et al., 2013; Pillon et al., 2014), which could be caused by hybridization, introgression, or incomplete lineage sorting.

Many relationships within and among other Cunonieae genera also varied across the ITS and plastid phylogenies. The monophyly of *Pterophylla* holds true in the plastid phylogeny (PP = 1.0), but not in the ITS tree. The differences with the target capture phylogeny (Pillon et al., 2021), the short branches, and non-perfect support for the node subtending *Pterophylla* (*Cunonia capensis*, *Pancheria*) (PP = 0.9) could be a signal of a hard polytomy at the stem of these three genera. In contrast, *Pancheria* remains monophyletic in our plastid and ITS trees; all *Pancheria* species occur in New Caledonia and are easily differentiated morphologically for their inflorescences in spherical capitula, dioecy, and whorled leaves (Hopkins et al., 2014).

Cunonia is not monophyletic under our denser sampling, with *C. capensis* placed as sister to *Pancheria* in the plastid tree (PP = 1.0, Fig. 1) and as sister to *Cunonia* + *Pancheria* (PP = 0.99) in the ITS tree (Fig. S3). Time calibration suggests that *C. capensis* has been isolated from the other members of *Cunonia* for about ~35 Myr. Morphological characters of *C. capensis* are more similar to those of New Caledonian *Cunonia* than *Pancheria* (although the shared characters between New Caledonian *Cunonia* and *C. capensis* might also be ancestral character states). For example, racemose inflorescences are present in *Cunonia* (including *C. capensis*), *Pterophylla*, and *Weinmannia*, but *Pancheria* and *Codia* have inflorescences of spherical heads (capitula). Accounting for the divergence of *C. capensis* from the other species of *Cunonia* at ~35 Ma, the disjunct distribution of the genus, and the fact that *C. capensis* is the type species of *Cunonia*, our results suggest that the New Caledonian *Cunonia* species might be considered as a different genus. Another plausible explanation is the intergeneric chloroplast capture between *Cunonia*, *Pancheria,* and *Pterophylla* through ancient hybridization and introgression (Tsitrone et al., 2003; Acosta & Premoli, 2010). Nevertheless, Pillon et al. (2021) retrieved a strong node support for the monophyletic *Cunonia*, with *Pancheria* as its sister group, based on many more nuclear genes, although with only two species: *C. capensis* and the New Caledonian *C. cerifera* Hoogland. The placement of *C. macrophylla* together with *C. capensis* in our ITS tree is weakly supported (PP = 0.49). *Cunonia macrophylla* is an early diverging taxon within *Cunonia* in our plastid tree and shares some morphological characters only with *C. schinziana* Däniker (but not with the remaining *Cunonia* species), including yellowish-green pendant flowers with stamen filaments more than five times as long as the corolla (Hopkins et al., 2014). The paraphyly of *Weinmannia* s.l. (sensu Bradford, 2002) is confirmed as well as the need to recognize *Weinmannia* and *Pterophylla* as different genera (Pillon et al., 2021, 2024).

4.2 Divergence times and changes in continental landmasses

In comparison with the time-calibration approach employed by Pillon et al. (2021), we based our calculations on a much broader taxon sampling so that we could include

well-studied fossils in Fagaceae, Salicaceae, and Rhamnaceae as further calibration points. This was possible due to a well-conserved plastid data set that provided a well-supported backbone phylogeny with representatives of related orders that also enhanced the resolution within Cunonieae (Figs. 1, S1, S3). Whereas the crown age of Cunoniaceae was similar between the present study (87.05 Ma, 88.9–80.5 Ma 95% HPD) and that of Pillon et al. (2021), which used nuclear sequence data of 14 loci from the Angiosperms353 bait set and a Yule′s (Birth only) branching process prior (88.6 Ma, ~93.1–84.1 Ma 95% HPD), the ages of Cunonieae and its genera inferred here are considerably older (Fig. 2; Table 1). The differences between the studies in the estimated ages of the Cunonieae may be related to differences in the rate of evolution between the plastid and the nuclear loci (Pillon et al., 2021). Another potential reason for the differences in divergence times is that our much denser Cunonieae taxon sampling may have led to older ages through a better representation of the tree space and internal branch lengths, accounting not only for diversification but also for lineage extinction. Finally, we used a BDM branching process prior and tested multiple scenarios of calibration (Table S4) based on carefully examined fossils spanning from the Cretaceous to the Miocene, together with the motif-alignment approach, which likely resulted in the best possible divergence-time estimation for the Cunonieae. We therefore argue that our older divergence time estimates are a reliable basis to evaluate biogeographic scenarios.

The major breakup event of the supercontinent Gondwana is considered to have occurred in the Early Jurassic (about 180 Ma), leading to the separation of West and East Gondwana (McLoughlin, 2001). The crown node age of Cunoniaceae was dated to after the breakup of Gondwana at ~87 Ma (Cretaceous), when South America was already separated from Africa, and India was distancing itself from Madagascar (McLoughlin, 2001). The fossil record of the family indicates that Cunoniaceae ancestors were also present in the proto-North American, European, and Asian continents, along with the Gondwanan landmasses (Tang et al., 2022). The Cenozoic started 66 Ma with a mass extinction event largely caused by the Chicxulub asteroid impact (Schulte et al., 2010), which mostly affected the northern hemisphere flora. Since that period, no fossils have been assigned to Cunoniaceae in the Northern Hemisphere. Therefore, extinction events in Laurasia and surviving lineages in Antarctica, Australia, and Patagonia are likely to have affected the distribution of Cunoniaceae during the Cenozoic (Schulte et al., 2010). During the Paleocene, the stem nodes of the tribes Geissoieae, Caldcluvieae, Codieae, and Cunonieae were present in Antarctica, South America, Australia, and Tasmania, which detached from Australia and Antarctica ~60 Ma (McLoughlin, 2001). Long branches during the Eocene and Oligocene may be the result of extinction events related with the AIS formation (Nge et al., 2020).

Then, Cunonieae experienced an increase in diversification during the Pliocene. The increase in the slope of the LTT plot from the Pliocene is explained by the initiation of diversification in New Caledonian *Cunonia* (crown node age 13.5 Ma, 22 extant species), *Pancheria* (crown node age 7.5 Ma, 25 extant species), Andean *Weinmannia* (crown node age 16.4 Ma, ~75 species), *Pterophylla* in Madagascar and Comoros (crown node age 5.2 Ma, ~38 species), and *Pterophylla* from Oceania (4.2 Ma, ~30 species). However, a more comprehensively sampled phylogeny at the species level is required to understand the diversification of *Pterophylla*. *Cunonia* and *Pancheria* mainly diversified in New Caledonia during the Pliocene after the final re-emergence of New Caledonia 25–34 Ma (Maurizot & Campbell, 2020). Our results suggest the occurrence of multiple events of colonization of New Caledonia by representatives of Cunonieae (*Cunonia, Pancheria*, and *Pterophylla*), followed by bursts of rapid diversification on the island. This has also been observed in other Cunoniaceae genera like *Codia* and *Geissois* (Pillon, Munzinger, et al., 2009b, Pillon et al., 2014). The potential factors driving the diversification of Cunoniaceae in New Caledonia need to be investigated in the future.

4.3 Antarctica′s role in shaping the current distribution of Cunonieae

Our hypothesis was that the expansion of the AIS expelled Cunonieae lineages from the Antarctic continent through extinction, leading to a gradual move and diversification of Cunonieae to its current distribution. The central geographical position of Antarctica makes it adjacent to the other land masses surrounding it: Australia, Tasmania, New Zealand, South America, and through a longer distance to Africa and Madagascar. This adjacency is key in explaining the past range expansions and vicariance events (de la Estrella et al., 2019). Before the formation of the AIS during the Eocene, the conditions were suitable for plants to occupy Antarctica and disperse to other land masses via ocean currents in the West Pacific that connected it with Patagonia, Southwest Africa, Tasmania, Australia, and New Zealand (Cantrill & Poole, 2012). Our results indicate that Cunonieae′s range included Antarctica and Patagonia during the Eocene and that Cunonieae likely dispersed from Antarctica, with one lineage (*Weinmannia*) reaching South America and the other lineage (*Cunonia*, *Pancheria*, and *Pterophylla*) dispersing to Tasmania, Australia, and Zealandia (Strogen et al., 2023).

During the Oligocene, the Drake Passage and the Tasman Seaway were important barriers leading to vicariance in Cunonieae. Through the Oligocene and Miocene, the AIS formation transformed Antarctica from an area of suitable habitat into a center of local extinctions (Truswell & Macphail, 2009). The AIS formation drove the Cunonieae lineages to extinction in Antarctica, producing a pattern of long branches in the plastid tree (Fig. 3), and greater extinction of ($e = 0.01833$) than the dispersal ($d = 0.0105$) in the DIVALIKE biogeographical reconstruction model, even when the jump dispersal was allowed (Table 2). Subsequently, one lineage (*Weinmannia*) likely dispersed from Patagonia to the Central Andes of Bolivia and the other lineage (*Cunonia*, *Pancheria*, and *Pterophylla*) through Australia (and Tasmania as indicated by the fossil of *Pterophylla* sp.) to Oceania and Malesia. Thus, New Caledonia and the tropical Andes would be considered "cradles" for *Cunonia*, *Pancheria*, and *Weinmannia* according to Stebbins′ (1974) definition or "incubators" using the terminology of Kuhnhäuser et al. (2025), whereas Australia (with two species of *Vesselowskya*), South Africa (with *C. capensis*), or Chile (with *W. trichosperma*) would be "museums" for

Cunonieae (Vasconcelos et al., 2022) or "accumulators" (Kuhnhäuser et al., 2025).

The biogeographic patterns recovered in the present study likely differ from those of previous studies because of the inclusion of fossils in our ancestral range reconstructions. We avoided possible biases in the ancestral range reconstruction toward the locations currently occupied by Cunonieae by also including fossil records that provided information on the Andean, Australian, North American, Patagonian, Tasmanian, and Antarctic distributions. The diversity of fossilized organs, from pollen, leaf fragments, or wood to complete infructescence or flowers, prevented the use of a "total-evidence" approach (Coiro et al., 2023). We constructed the BioGeoBEARS time-stratified model based on consensus palaeogeographical information about the history of tectonics in the Southern Hemisphere and particularly in Antarctica (Cantrill & Poole, 2012). We conclude that the role of Antarctica was pivotal for the origin of the Cunonieae tribe. The previous work of Pillon et al. (2021) did not recover that pattern in their biogeography reconstruction because it did not include Antarctic fossils in the analysis; therefore, their BioGeoBEARS model was not informed about the past distribution on that continent.

4.4 Processes affecting patterns of diversity in Cunonieae

This first densely sampled phylogeny has also clarified biogeographical patterns in *Weinmannia*. *Weinmannia* first colonized southern South America and, through a process of migration and diversification, migrated from the temperate forests of Chile to the Yungas in Bolivia and to the Cloud Forest of Central Andes during the Miocene (~14.5 Ma). During this time, the process of Andean uplift resulted in intense drought in lowland areas, producing the South American Dry Diagonal (SADD) (Luebert, 2021), which likely became a barrier between tropical and extratropical *Weinmannia* in the Miocene. *Weinmannia* then colonized the Northern Andes during the Pliocene (~5.7 Ma), following a pattern of dispersal from South to North (see also Segovia et al., 2024, preprint). Also, the Andes probably became a source for more recent dispersal of *Weinmannia* to other biomes: the Guyana Shield, Atlantic Forest in Brazil, Central America, and Caribbean islands, which can be tested in the future with a sampling focused on these areas. The polytomies among Central and Northern Andes *Weinmannia* species might indicate recent diversification, incomplete lineage sorting, and possible hybridization/introgression events. Other taxa of hybrid origin have been described within the tribe Cunonieae, for example, *Cunonia* × *alticola* Guillaumin or *Pancheria* × *heterophylla* Vieill. ex Guillaumin (Hopkins et al., 2014), and in other Cunoniaceae like the genus *Spiraeanthemum* (Pillon and Hopkins et al., 2009a) or *Codia* (Pillon and Munzinger et al., 2009b). However, employing denser taxon sampling and an increased number of DNA characters (e.g., generated with RAD-seq, sequence capture, or genome skimming) is necessary to further disentangle relationships among South American *Weinmannia* in the last ~15 Myr.

Although several other Cunoniaceae reached South America, none are as diverse as *Weinmannia*, which could have several different underlying causes. Along with *Weinmannia*, three other genera of Cunoniaceae reached South America: *Caldcluvia* D.Don (one species), *Eucryphia* Cav. (two species), and *Lamanonia* Vell. (six species from Brazil). These are not present in the Tropical Andes; *Caldcluvia* and *Eucryphia* only share distribution ranges with *W. trichosperma* from Chile and Argentina. In comparison with *Caldcluvia*, *Eucryphia*, and *Lamanonia*, the success of *Weinmannia* in the Tropical Andes (>70 spp.) relies at least in part on their ability to colonize steep slopes and open and unstable terrains, which are associated with areas that have cloud condensation (Montes Pulido, 2011; Derroire et al., 2007), orogenic processes, and a history of volcanism (Hopkins & Bradford, 1998; Morales, 2010). Interestingly, *Pterophylla* is also a typical component of cloud forests with volcanic history in many Pacific islands, the Comoros, and some parts of Malesia, as is *Weinmannia* in the volcanic mountains of the Mascarenes (Mueller-Dombois & Fosberg, 1998). Another process that may have led to higher diversification in *Weinmannia* relative to the other Cunonieae genera in South America is elevational fluctuations in climate in the central and northern Andes caused by glacial and interglacial periods during the Pleistocene, which acted as a driver of speciation because it led to the isolation and reconnection of populations over cycles of thousands of years (Nevado et al., 2018), Finally, several traits related to migration may be responsible for the greater range of habitats occupied by *Weinmannia*; for example, Pérez et al. (2009) detected pollen of *W. trichosperma* dispersed from a source at least 127 km away across the Andes. *Weinmannia* seeds are very small, light, and hairy, often germinating in tree-fern trunks (Derroire et al., 2007); however, little is known about *Weinmannia* or Cunonieae dispersal mechanisms.

Another interesting question regards several genera that exhibit large disjunctions in their distributions, such as *C. capensis* in South Africa and *W. tinctoria* (and *W. mauritiana*) in the Mascarenes. The current disjunct distribution could be explained as long-distance dispersal events in the Miocene in the case of *C. capensis* and in the late Oligocene in the case of *W. tinctoria*. But would these jump dispersals have happened directly from New Caledonia to South Africa? or from the Mascarenes to Patagonia? and in what direction? These are questions that require further investigation.

The parameters of our DIVALIKE model of ancestral range reconstruction did not allow the long-distance dispersal, with $j = 0.0$ (jump dispersal). It allowed the dispersal only between adjacent areas, explicitly given to the model via a matrix of area adjacency, with a resulting value of d (dispersal) = 0.0105 (Table 2). Another possible explanation for the current disjunct distribution is that ancient vicariance gave rise to both, involving both low diversification/extinction scenarios (LDE) and high diversification/extinction scenarios (HDE). For example, in *Cunonia* and *Pancheria*, a South Africa LDE scenario could have given rise to *C. capensis* in contrast to the New Caledonia HDE scenario of the remaining *Cunonia* and *Pancheria*. Another example in *Weinmannia* involves an LDE scenario in the Pacific forests of Chile (*W. trichosperma*) and the Mascarene Islands (*W. tinctoria*) versus a HDE scenario of the Tropical Andes *Weinmannia*. Vicariance could have played a role between Chile and the Central Andes *Weinmannia* if ancestral populations were disconnected by the establishment of the SADD as a biogeographical barrier (Luebert, 2021). The study of the evolutionary history of some central Andes

species related to the Chilean *W. trichosperma*, such as *W. boliviensis*, *W. crassifolia*, or *Weinmannia geometrica* Rusby, could shed light on this intracontinental disjunction. These old disconnections could also explain the relatively long branches of the taxa under LDE scenarios. In a LDE scenario like South Africa, there is almost no orogeny or recent volcanic activity, nor mountains with cloud forest, while in a HDE scenario such as Madagascar, this niche has been occupied by ca. 40 species of *Pterophylla* (Bradford, 2001).

In summary, the results of our study indicate that Cunonieae likely originated in the Antarctic and dispersed to other regions in the southern hemisphere. Then, the Oligocene and Miocene extinctions of Cunonieae in the Antarctic, largely caused by the AIS formation, led to the current disjunct distribution of *Weinmannia* in the Mascarenes and the Americas and to the arrival and diversification of *Cunonia* and *Pancheria* in New Caledonia. Finally, the Andean radiation of *Weinmannia*, occurring since the late Miocene, was potentiated by the Andean uplift.

Acknowledgements

We would like to thank Alexander Linan, Astrid De Mestier, Belen Escobari, Eduardo Aguirre, Iván Jimenez, Juan Penagos, Konstantina Koutroumpa, Kim Govers, Monica Carlsen, Nadja Korotkova, Nils Köster, and William Farfan-Rios for discussing methods and results. For their help during the fieldwork, we thank Álvaro Idárraga, Andrea Chaspuengal, Boris Villanueva, Cristian Castro, Daniel Franco, David Bruy, Diego Cabrera, Dubán Canal, Érika Benavides, Gloria Gutiérrez, Gustavo Loboguerrero, Gustavo Silva, Lina Corrales, Moisés Penagos, Paola Peña, Tatiana Montilla, Yeison Montoya, and Yulieth Ávila. Thanks to herbarium curators Juraj Paule (B), Jordan Teisher (MO), and Myriam Gaudeul (P). The Ph.D. project of the first author was funded by the Botanical Garden Berlin, Freie Universität Berlin, in the context of the collaboration with the Jardin Botánico José Celestino Mutis in Bogotá (Colombia) through the project number 03008 "Evolution and biogeography of the genus *Weinmannia* (Cunoniaceae)." Further support came from the *Weinmannia* project at the Missouri Botanical Garden, FONDECYT 11200967, the National Science Foundation grant DEB1836353, Instituto de Ecología y Biodiversidad ANID grant FB210006, and botanical gardens of Bogotá and Medellín in Colombia. We thank the Ministerio del Ambiente, Agua y Transición Ecológica in Ecuador for collecting permits (Contrato marco MAE-DNB-CM-2019-011) and the Autoridad Nacional de Licencias Ambientales–ANLA in Colombia for issuing the exportation permits 02761 of 2022 and 3279 of 2023. Open Access funding enabled and organized by Projekt DEAL.

Author Contributions

Francisco Fajardo-Gutiérrez, James E. Richardson, Thomas Borsch, Christine E. Edwards, Sebastian Tello, Yohan Pillon, conceived the ideas and designed the study; Francisco Fajardo-Gutiérrez, Alfredo Fuentes, Christine E. Edwards, Mariasole Calbi, Nora H. Oleas, Ricardo A. Segovia and Sebastian Tello conducted the fieldwork and collected the data with additional material from collaborators; Francisco Fajardo-Gutiérrez, Markus S. Dillenberger and Thomas Borsch performed laboratory and data analyses; and Francisco Fajardo-Gutiérrez led the writing with assistance from Christine E. Edwards, Mariasole Calbi, James E. Richardson, Nora H. Oleas, Ricardo A. Segovia, Yohan Pillon, and Thomas Borsch. All the authors agreed with the content of the manuscript.

Conflicts of Interest

The authors declare no conflict of interest.

Data Availability Statement

We generated new 402 sequences from 104 samples of Cunoniaceae. These sequences have been submitted to GenBank, and accession numbers are listed in Table S1. Research data consisting of plastid and nuclear alignments (ITS), intermediate tree files, executable scripts, and parameters for phylogenetic analyses, molecular time calibration in BEAST, and ancestral range reconstruction in BioGeoBEARS are available in Figshare (Fajardo, 2024a, 2024b, 2024c).

References

Acosta MC, Premoli AC. 2010. Evidence of chloroplast capture in south American *Nothofagus* (subgenus *Nothofagus*, Nothofagaceae). *Molecular Phylogenetics and Evolution* 54: 235–242.

Anderson JM, Anderson HM, Archangelsky S, Bamford M, Chandra S, Dettmann M, Hill R, McLoughlin S, Rösler O. 1999. Patterns of Gondwana plant colonisation and diversification. *Journal of African Earth Sciences* 28: 145–167.

Barker NP, Weston PH, Rutschmann F, Sauquet H. 2007. Molecular dating of the "Gondwanan" plant family Proteaceae is only partially congruent with the timing of the break-up of Gondwana. *Journal of Biogeography* 34: 2012–2027.

Barnes RW. 1999. *Palaeobiogeography, extinctions and evolutionary trends in the Cunoniaceae: A synthesis of the fossil record*. Doctoral Dissertation. Tasmania, Australia: University of Tasmania. https://doi.org/10.25959/23246864.v1

Barnes RW, Hill RS, Bradford JC. 2001. The history of Cunoniaceae in Australia from macrofossil evidence. *Australian Journal of Botany* 49: 301–320.

Bartish IV, Antonelli A, Richardson JE, Swenson U. 2011. Vicariance or long-distance dispersal: Historical biogeography of the pantropical subfamily Chrysophylloideae (Sapotaceae). *Journal of Biogeography* 38: 177–190.

Bartish IV, Swenson U, Munzinger J, Anderberg AA. 2005. Phylogenetic relationships among New Caledonian Sapotaceae (Ericales): Molecular evidence for generic polyphyly and repeated dispersal. *American Journal of Botany* 92: 667–673.

Bennett L, Melchers B, Proppe B. 2020. *Curta: A general-purpose high-performance computer at ZEDAT*. Berlin, Germnay: Freie Universität Berlin. https://doi.org/10.17169/refubium-26754

Borsch T, Hilu KW, Quandt D, Wilde V, Neinhuis C, Barthlott W. 2003. Noncoding plastid trnT–trnF sequences reveal a well resolved phylogeny of basal angiosperms. *Journal of Evolutionary Biology* 16: 558–576.

Boschman LM. 2021. Andean mountain building since the Late Cretaceous: A paleoelevation reconstruction. *Earth-Science Reviews* 220: 103640.

Bouckaert RR, Drummond AJ. 2017. bModelTest: Bayesian phylogenetic site model averaging and model comparison. *BMC Evolutionary Biology* 17: 1–11.

Bouckaert R, Vaughan TG, Barido-Sottani J, Duchêne S, Fourment M, Gavryushkina A, Heled J, Jones G, Kühnert D, De Maio N, Matschiner M, Mendes FK, Müller NF, Ogilvie HA, du Plessis L, Popinga A, Rambaut A, Rasmussen D, Siveroni I, Suchard MA, Wu C-H, Xie D, Zhang C, Stadler T, Drummond AJ. 2019. BEAST 2.5: An advanced software platform for Bayesian evolutionary analysis. *PLoS Computational Biology* 15: 1006650.

Bradford JC. 1998. A cladistic analysis of species groups in *Weinmannia* (Cunoniaceae) based on morphology and inflorescence architecture. *Annals of the Missouri Botanical Garden* 85: 565–593.

Bradford JC. 2001. The application of a cladistic analysis to the classification and identification of *Weinmannia* (Cunoniaceae) in Madagascar and the Comoro Islands. *Adansonia* 23: 237–246.

Bradford JC. 2002. Molecular phylogenetics and morphological evolution in Cunonieae (Cunoniaceae). *Annals of the Missouri Botanical Garden* 89: 491–503.

Bradford JC, Barnes RW. 2001. Phylogenetics and classification of Cunoniaceae (Oxalidales) using chloroplast DNA sequences and morphology. *Systematic Botany* 26: 354–385.

Campagna ML, Downie SR. 1998. The intron in chloroplast gene rpl16 is missing from the flowering plant families Geraniaceae, Goodeniaceae, and Plumbaginaceae. *Transactions of the Illinois State Academy of Science* 91: 1–11.

Cantrill DJ, Poole I. 2012. *The vegetation of Antarctica through geological time*. Cambridge: Cambridge University Press.

Chacón J, de Assis MC, Meerow AW, Renner SS. 2012. From east Gondwana to Central America: historical biogeography of the Alstroemeriaceae. *Journal of Biogeography* 39: 1806–1818.

Coiro M, Allio R, Mazet N, Seyfullah LJ, Condamine FL. 2023. Reconciling fossils with phylogenies reveals the origin and macroevolutionary processes explaining the global cycad biodiversity. *New Phytologist* 240: 1616–1635.

Cruaud A, Jabbour-Zahab R, Genson G, Ungricht S, Rasplus JY. 2012. Testing the emergence of New Caledonia: Fig wasp mutualism as a case study and a review of evidence. *PLoS One* 7: 30941.

Derroire G, Schmitt L, Rivière JN, Sarrailh JM, Tassin J. 2007. The essential role of tree-fern trunks in the regeneration of *Weinmannia tinctoria* in rain forest on Réunion, Mascarene Archipelago. *Journal of Tropical Ecology* 23: 487–492.

Drummond AJ, Rambaut A. 2007. Tree Annotator, version 2.6.0 [online]. Available from http://beast.bio.ed.ac.uk [accessed 30 August 2020].

Drummond AJ, Ho SYW, Phillips MJ, Rambaut A. 2006. Relaxed phylogenetics and dating with confidence. *PLoS Biology* 4: 88.

Duchêne D, Duchêne S, Ho SY. 2015. Tree imbalance causes a bias in phylogenetic estimation of evolutionary timescales using heterochronous sequences. *Molecular Ecology Resources* 15: 785–794.

de la Estrella MDL, Buerki S, Vasconcelos T, Lucas EJ, Forest F. 2019. The role of Antarctica in biogeographical reconstruction: a point of view. *International Journal of Plant Sciences* 180: 63–71.

Fajardo F. 2024a. Cunonieae Phylogenetic Analyses. figshare. Dataset [online]. Available from https://doi.org/10.6084/m9.figshare.27641577 [accessed 3 December 2024].

Fajardo F. 2024b. Cunonieae time calibration. figshare. Journal contribution [online]. Available from https://doi.org/10.6084/m9.figshare.27641676 [accessed 3 December 2024].

Fajardo F. 2024c. Cunonieae ancestral range reconstruction. figshare. Journal contribution [online]. Available from https://doi.org/10.6084/m9.figshare.27641679 [accessed 3 December 2024].

Foster CS, Sauquet H, Van der Merwe M, McPherson H, Rossetto M, Ho SY. 2017. Evaluating the impact of genomic data and priors on Bayesian estimates of the angiosperm evolutionary timescale. *Systematic Biology* 66: 338–351.

González-Caro S, Tello JS, Myers JA, Feeley K, Blundo C, Calderón-Loor M, Carilla J, Cayola L, Cuesta F, Farfán W, Fuentes AF, Garcia-Cabrera K, Grau R, Idárraga A, Loza MI, Malhi Y, Malizia A, Malizia L, Osinaga-Acosta O, Pinto E, Salinas N, Silman M, Terán-Valdéz A, Duque Á. 2023. Historical assembly of Andean tree communities. *Plants* 12: 3546.

Hopkins HCF, Bradford JC. 1998. A revision of *Weinmannia* (Cunoniaceae) in Malesia and the Pacific 1. Introduction and an account of the species of Western Malesia, the Lesser Sunda Islands and the Moluccas. *Adansonia* 20: 5–41.

Hopkins HCF, Pillon Y, Hoogland RD 2014. Flore de la Nouvelle-Calédonie 26: Cunoniaceae. Marseille: Publications scientifiques du Museum, Paris/IRD Éditions.

Hopkins HCF, Rozefelds AC, Pillon Y. 2013. *Karrabina* gen. nov. (Cunoniaceae), for the Australian species previously placed in *Geissois*, and a synopsis of genera in the tribe Geissoieae. *Australian Systematic Botany* 26: 167–185.

Inglis PW, Pappas MDCR, Resende LV, Grattapaglia D. 2018. Fast and inexpensive protocols for consistent extraction of high quality DNA and RNA from challenging plant and fungal samples for high-throughput SNP genotyping and sequencing applications. *PloS One* 13: 0206085.

Johnson MG, Pokorny L, Dodsworth S, Botigué LR, Cowan RS, Devault A, Eiserhardt WF, Epitawalage N, Foster F, Kim JT, Leebens-Mack JH, Leitch IJ, Maurin O, Soltis DE, Soltis PS, Wong GK, Baker WJ, Wickett NJ. 2019. A universal probe set for targeted sequencing of 353 nuclear genes from any flowering plant designed using k-medoids clustering. *Systematic Biology* 68: 594–606.

Jokat W, Boebel T, König M, Meyer U. 2003. Timing and geometry of early Gondwana breakup. Journal of Geophysical Research: Solid Earth 108: 1–15. https://doi.org/10.1029/2002JB001802

Kennedy AT, Farnsworth A, Lunt DJ, Lear CH, Markwick PJ. 2015. Atmospheric and oceanic impacts of Antarctic glaciation across the Eocene–Oligocene transition. *Philosophical Transactions of the Royal Society A: Mathematical, Physical and Engineering Sciences* 373: 20140419.

Kozlov AM, Darriba D, Flouri T, Morel B, Stamatakis A. 2019. RAxML-NG: A fast, scalable and user-friendly tool for maximum likelihood phylogenetic inference. *Bioinformatics* 35: 4453–4455.

Kuhnhäuser BG, Bates CD, Dransfield J, Geri C, Henderson A, Julia S, Lim JY, Morley RJ, Rustiami H, Schley RJ, Bellot S. 2025. Island geography drives evolution of rattan palms in tropical Asian rainforests. *Science* 387: 1204–1209.

Lartillot N, Philippe H. 2006. Computing Bayes factors using thermodynamic integration. *Systematic Biology* 55: 195–207.

Lemoine F, Domelevo Entfellner JB, Wilkinson E, Correia D, Dávila Felipe M, De Oliveira T, Gascuel O. 2018. Renewing Felsenstein's phylogenetic bootstrap in the era of big data. *Nature* 556: 452–456.

León B. 2006. Cunoniaceae endémicas del Perú. *Revista Peruana de Biología* 13: 275–276.

Li X, Zhao Y, Tu X, Li C, Zhu Y, Zhong H, Liu Z-J, Wu S, Zhai J. 2021. Comparative analysis of plastomes in Oxalidaceae: Phylogenetic

relationships and potential molecular markers. *Plant Diversity* 43: 281–291.

Liu B, Le CT, Barrett RL, Nickrent DL, Chen Z, Lu L, Vidal-Russell R. 2018. Historical biogeography of Loranthaceae (Santalales): Diversification agrees with emergence of tropical forests and radiation of songbirds. *Molecular Phylogenetics and Evolution* 124: 199–212.

Löhne C, Borsch T. 2005. Molecular evolution and phylogenetic utility of the *petD* group II intron: A case study in basal angiosperms. *Molecular Biology and Evolution* 22: 317–332.

Luebert F. 2021. The two South American dry diagonals. *Frontiers of Biogeography* 13: 51267.

Madriñán S, Cortés AJ, Richardson JE. 2013. Páramo is the world's fastest evolving and coolest biodiversity hotspot. *Frontiers in Genetics* 4: 192.

Martin W, Deusch O, Stawski N, Grünheit N, Goremykin V. 2005. Chloroplast genome phylogenetics: Why we need independent approaches to plant molecular evolution. *Trends in Plant Science* 10: 203–209.

Matel TP, Gandolfo MA, Hermsen EJ, Wilf P. 2022. Cunoniaceae infructescences from the early Eocene Laguna del Hunco flora, Patagonia, Argentina. *American Journal of Botany* 109: 986–1003.

Matzke NJ. 2013. BioGeoBEARS: BioGeography with Bayesian (and likelihood) evolutionary analysis in R Scripts. R package, version 0.2.1 [online]. Available from http://CRAN.R-project.org/package=BioGeoBEARS [accessed 20 May 2024].

Matzke NJ. 2014. Model selection in historical biogeography reveals that founder-event speciation is a crucial process in island clades. *Systematic Biology* 63: 951–970.

Maurizot P, Campbell HJ. 2020. Chapter 8 Palaeobiogeography of New Caledonia. *Geological Society, London, Memoirs* 51: 189–213.

Mays C, Tosolini AMP, Cantrill DJ, Stilwell JD. 2015. Late Cretaceous (Cenomanian–Turonian) macroflora from the Chatham Islands, New Zealand: Bryophytes, lycophytes and pteridophytes. *Gondwana Research* 27: 1042–1060.

McLoughlin S. 2001. The breakup history of Gondwana and its impact on pre-Cenozoic floristic provincialism. *Australian Journal of Botany* 49: 271–300.

Milner ML, Weston PH, Rossetto M, Crisp MD. 2015. Biogeography of the Gondwanan genus *Lomatia* (Proteaceae): Vicariance at continental and intercontinental scales. *Journal of Biogeography* 42: 2440–2451.

Montes Pulido CR. 2011. Estado del conocimiento en *Weinmannia tomentosa* L.f. (encenillo) y algunas propuestas de estudio sobre su regeneración. *Revista de Investigación Agraria y Ambiental* 2: 45–53.

Morales JF 2010. Synopsis of the genus *Weinmannia* (Cunoniaceae) in Mexico and Central America. Anales del Jardín Botánico de Madrid 67: 137–155.

Mueller-Dombois D, Fosberg FR. 1998. *Vegetation of the tropical Pacific islands*. New York: Springer Science & Business Media.

Müller KF. 2004. PRAP—computation of Bremer support for large data sets. *Molecular Phylogenetics and Evolution* 31: 780–782.

Müller KF. 2005a. SeqState-primer design and sequence statistics for phylogenetic DNA data sets. *Applied Bioinformatics* 4: 65–69.

Müller KF. 2005b. The efficiency of different search strategies in estimating parsimony jackknife, bootstrap, and Bremer support. *BMC Evolutionary Biology* 5: 58.

Müller K, Quandt D, Müller J, Neinhuis C. 2005. PhyDE, Version 0.92: Phylogenetic data editor [online]. Available from http://phyde.de [accessed August 2020].

Nattier R, Pellens R, Robillard T, Jourdan H, Legendre F, Caesar M, Nel A, Grandcolas P. 2017. Updating the phylogenetic dating of New Caledonian biodiversity with a meta-analysis of the available evidence. *Scientific Reports* 7: 3705.

Nevado B, Contreras-Ortiz N, Hughes C, Filatov DA. 2018. Pleistocene glacial cycles drive isolation, gene flow and speciation in the high-elevation Andes. *New Phytologist* 219: 779–793.

Nge FJ, Biffin E, Thiele KR, Waycott M. 2020. Extinction pulse at Eocene–Oligocene boundary drives diversification dynamics of two Australian temperate floras. *Proceedings of the Royal Society B* 287: 20192546.

Paradis E, Schliep K. 2019. ape 5.0: An environment for modern phylogenetics and evolutionary analyses in R. *Bioinformatics* 35: 526–528.

Pérez cf, Castañeda ME, Gassmann MI, Bianchi MM. 2009. A statistical study of *Weinmannia* pollen trajectories across the Andes. *Advances in Geosciences* 22: 79–84.

Pillon Y. 2012. Time and tempo of diversification in the flora of New Caledonia. *Botanical Journal of the Linnean Society* 170: 288–298.

Pillon Y, Crayn D, Streiff SJR, De Vos JM. 2024. A suprageneric classification of Oxalidales. *Swainsona* 38: 153–160.

Pillon Y, Hopkins HC, Maurin O, Epitawalage N, Bradford J, Rogers ZS, Baker WJ, Forest F. 2021. Phylogenomics and biogeography of Cunoniaceae (Oxalidales) with complete generic sampling and taxonomic realignments. *American Journal of Botany* 108: 1181–1200.

Pillon Y, Hopkins HFC, Munzinger J, Amir H, Chase MW. 2009a. Cryptic species, gene recombination and hybridization in the genus *Spiraeanthemum* (Cunoniaceae) from New Caledonia. *Botanical Journal of the Linnean Society* 161: 137–152.

Pillon Y, Hopkins HC, Rigault F, Jaffré T, Stacy EA. 2014. Cryptic adaptive radiation in tropical forest trees in New Caledonia. *New Phytologist* 202: 521–530.

Pillon Y, Munzinger J, Amir H, Hopkins HFC, Chase MW. 2009b. Reticulate evolution on a mosaic of soils: Diversification of the New Caledonian endemic genus *Codia* (Cunoniaceae). *Molecular Ecology* 18: 2263–2275.

Pujana RR, Iglesias A, Raffi ME, Olivero EB. 2018. Angiosperm fossil woods from the upper cretaceous of western Antarctica (Santa Marta Formation). *Cretaceous Research* 90: 349–362.

Pujana RR, Santelli MB, Alvarez MJ, Raffi ME, Santillana SN. 2025. Angiosperm fossil woods, Cryptocaryeae (Lauraceae) and Cunoniaceae, with marine borers from Day Nunatak, Western Antarctica (Snow Hill Island Formation, Upper Cretaceous). *Cretaceous Research* 174: 106146.

Quiroga MP, Mathiasen P, Iglesias A, Mill RR, Premoli AC. 2016. Molecular and fossil evidence disentangle the biogeographical history of *Podocarpus*, a key genus in plant geography. *Journal of Biogeography* 43: 372–383.

Rambaut A, Drummond AJ, Xie D, Baele G, Suchard MA. 2018. Posterior summarization in Bayesian phylogenetics using Tracer 1.7. *Systematic Biology* 67: 901–904.

Raven PH, Axelrod DI. 1972. Plate tectonics and Australasian paleobiogeography: The complex biogeographic relations of the region reflect its geologic history. *Science* 176: 1379–1386.

Ree RH, Sanmartín I. 2018. Conceptual and statistical problems with the DEC+ J model of founder-event speciation and its comparison with DEC via model selection. *Journal of Biogeography* 45: 741–749.

Ronquist F, Teslenko M, Van Der Mark P, Ayres DL, Darling A, Höhna S, Larget B, Liu L, Suchard MA, Huelsenbeck JP. 2012. MrBayes

3.2: Efficient Bayesian phylogenetic inference and model choice across a large model space. *Systematic Biology* 61: 539–542.

Rossetto-Harris G, Wilf P, Escapa IH, Andruchow-Colombo A. 2020. Eocene *Araucaria* sect. *Eutacta* from Patagonia and floristic turnover during the initial isolation of South America. *American Journal of Botany* 107: 806–832.

Schulte P, Alegret L, Arenillas I, Arz JA, Barton PJ, Bown PR, Bralower TJ, Christeson GL, Claeys P, Cockell CS, Collins GS, Deutsch A, Goldin TJ, Goto K, Grajales-Nishimura JM, Grieve RAF, Gulick SPS, Johnson KR, Kiessling W, Koeberl C, Kring DA, MacLeod KG, Matsui T, Melosh J, Montanari A, Morgan JV, Neal CV, Nichols DJ, Norris RD, Pierazzo E, Ravizza G, Rebolledo-Vieyra M, Reimold WU, Robin E, Salge T, Speijer RP, Sweet AR, Urrutia-Fucugauchi J, Vajda V, Whalen MT, Willumsen PS. 2010. The Chicxulub asteroid impact and mass extinction at the Cretaceous-Paleogene boundary. *Science* 327: 1214–1218.

Segovia RA, Armesto JJ. 2015. The Gondwanan legacy in South American biogeography. *Journal of Biogeography* 42: 209–217.

Simmons MP, Ochoterena H. 2000. Gaps as characters in sequence-based phylogenetic analyses. *Systematic Biology* 49: 369–381.

Stebbins GL. 1974. *Flowering plants: Evolution above the species level*. Cambridge, MA: Harvard University Press. https://doi.org/10.4159/harvard.9780674864856.

Stöver BC, Müller KF. 2010. TreeGraph 2: Combining and visualizing evidence from different phylogenetic analyses. *BMC bioinformatics* 11: 1–9.

Strogen DP, Seebeck H, Hines BR, Bland KJ, Crampton JS. 2023. Palaeogeographic evolution of Zealandia: Mid-Cretaceous to present. *New Zealand Journal of Geology and Geophysics* 66: 528–557.

Swofford DL. 2002. *PAUP: Phylogenetic analysis using parsimony (and other methods), version 4*. Sunderland, MA: Sinauer.

Taberlet P, Gielly L, Pautou G, Bouvet J. 1991. Universal primers for amplification of three non-coding regions of chloroplast DNA. *Plant Molecular Biology* 17: 1105–1109.

Tang KK, Smith SY, Atkinson BA. 2022. Extending beyond Gondwana: Cretaceous Cunoniaceae from western North America. *New Phytologist* 234: 704–718.

Thiers BM 2025 (updated continuously). Index Herbariorum. https://sweetgum.nybg.org/science/ih/

Truswell EM, Macphail MK. 2009. Polar forests on the edge of extinction: what does the fossil spore and pollen evidence from East Antarctica say? *Australian Systematic Botany* 22: 57–106.

Tsitrone A, Kirkpatrick M, Levin DA. 2003. A model for chloroplast capture. *Evolution* 57: 1776–1782.

Vasconcelos T, O'Meara BC, Beaulieu JM. 2022. Retiring "cradles" and "museums" of biodiversity. *The American Naturalist* 199: 194–205.

Vento B, Agrain F, Puebla G. 2024. Ancient Antarctica: The early evolutionary history of *Nothofagus*. *Historical Biology* 36: 136–146.

Wang Y, Xie Y, Jin J, Li J, Qiu X, Tong Y, Li Z, Zhang Z, Lai W. 2023. Comparison of the chloroplast genomes and phylogenomic analysis of Elaeocarpaceae. *PeerJ* 11: e15322.

White TJ, Bruns T, Lee SJWT, Taylor J. 1990. Amplification and direct sequencing of fungal ribosomal RNA genes for phylogenetics. *PCR protocols: A Guide to Methods and Applications* 18: 315–322.

Wicke S, Quandt D. 2009. Universal primers for the amplification of the plastid *trnK/matK* region in land plants. *Anales del Jardín Botánico de Madrid* 66: 285–288.

Wood HM, Matzke NJ, Gillespie RG, Griswold CE. 2013. Treating fossils as terminal taxa in divergence time estimation reveals ancient vicariance patterns in the palpimanoid spiders. *Systematic Biology* 62: 264–284.

Zuntini AR, Carruthers T, Maurin O, Bailey PC, Leempoel K, Brewer GE, Epitawalage N, Françoso E, Gallego-Paramo B, McGinnie C, Negrão R. 2024. Phylogenomics and the rise of the angiosperms. *Nature* 629: 843–850.

Supplementary Material

The following supplementary material is available online for this article at http://onlinelibrary.wiley.com/doi/10.1111/jse.70004/suppinfo:

Fig. S1. Map with the distribution of 127 Cunoniaceae samples used in this study for the plastid phylogenetic trees, of which 116 correspond to new generated DNA sequences (red dots) and 11 were data obtained from GenBank (blue dots). *Pa.* = *Pancheria*, *Pter.* = *Pterophylla*.

Fig. S2. Continuation of Fig. 1 of the main text. Phylogeny of the Cunoniaceae and external groups based on concatenated sequences of *matK*, *trnL-F* and *rpL-16* plastid markers. PP = posterior probability, TBE = Transfer Bootstrap Expectation, and JK = Jackknife. CELAS = Celastrales, CUCUR = Cucurbitales, FABAL = Fabales, FAGAL = Fagales, MALPIG = Malpighiales, and ROSAL = Rosales, ZYGO = Zygophyllales. Scientific names of Cunoniaceae samples are followed by two letters representing the Alpha-2 code of the country of the collection event according to the ISO 3166 international standard.

Fig. S3. Phylogenetic relationships of the Cunonieae based on the nuclear ITS sequences of 86 taxa. Support values are given on the subtending branch of each node: on top PP = posterior probability [bold], and TBE = Transfer Bootstrap Expectation [italics], and JK = Jackknife below the line. The topology shown resulted from the Bayesian analysis; support values in square brackets were not identically recovered by the maximum likelihood or the parsimony analyses. The two letters at the end of the scientific names are Alpha-2 code of the country of the collection event following the ISO 3166 international standard.

Fig. S4. Time calibration of Cunoniaceae crown node with a reduced sampling (65 tips) with a balance topology and to allow to include nine Rosid fossil calibration points (yellow stars) of the scenario A in supporting Table S4. Names and ages of fossil calibration points are described in the Table S3.

Fig. S5. Comparison between plastid markers tree (at the left side) and nuclear ITS tree (at the right side) for Cunonieae tribe. Linking black lines are drawn between the same exact samples on both trees, dashed lines link the same species but different samples, and red lines show three remarkable different placements. Nodes were rotated to facilitate the visualization. Complete list of samples and vouchers can be found in Table S1.

Fig. S6. Summary of the phylogenetic incongruences between the plastid markers and the nuclear ITS trees inside the Cunonieae tribe. The supports values are posterior probabilities, and the dashed circles show nodes that are Not present in the other tree at a genus level. *Pt.* = *Pterophylla*; the Alpha-2 code of each country was used to describe the distribution of the tips and collapsed clades, following the ISO 3166 international standard.

Table S1. Taxa and accessions included in phylogenetic analyses for the *trnK-matK*, *trnL-trnF*, *rps3-rpL16* and nuclear ribosomal ITS DNA regions. In alphabetical order of scientific names, locality and voucher information are given for newly generated sequences, and references for the GenBank accessions.

Table S2. Nucleotide substitution models. Evolutionary models selected based on the AIC for each partition, position, and lengths numbers after removing mutational hot spots of the reduced phylogenetic matrix of 130 samples used for the time calibration analysis.

Table S3. Fossil records used as calibration points for divergence time estimation of Cunonieae; lower bound of prior (LBP) or minimum age, and upper bound of prior (UBP) as used in BEAST2.

Table S4. Summary of the main time-calibration scenarios explored.

Table S5. Fossil records of Cunoniaceae used in the ancestral area reconstruction.

Table S6. BioGeoBEARS tips data file, 94 taxa and 14 areas. Area coding: Antarctic=A, Australia=B, Tasmania=C, New Zealand=D, Malesia and New Guinea=E, New Caledonia=F, Patagonia=G, Central Andes=H, Brazil=I, Northern Andes=J, North America=K, South Africa=L, Madagascar=M, Reunion, Samoa & Comoros=N.

Table S7. Thresholds for the time stratified analysis in BioGeoBEARS in million years.

Table S8. Areas allowed matrix for time stratified analysis in BioGeoBEARS. Coding as in Table S6.

Table S9. Dispersal multipliers matrix for the time stratified analysis in BioGeoBEARS, the probability of dispersal events between two areas based on the approach of de la Estrella (2019). Coding as in Table S6.

Table S10. Areas adjacency matrix for the time stratified analysis in BioGeoBEARS, 0 values indicate non adjacent areas accounting for intercontinental proximity. Coding as in Table S6.

Table S11. Comparative tests of the BioGeoBEARS models.